Time-Resolved Photodissociations of Iodotoluene Radical Cations†

Byungjoo Kim‡ and Seung Koo Shin*,§

Division of Chemistry and Radiation, Korea Research Institute of Standards and Science, P.O. Box 102, Yusong, Taejon, Korea 305-600, and FT-ICR Laboratory, Department of Chemistry, Pohang University of Science and Technology, San31 Hyojadong Namgu, Pohang, Kyungbuk, Korea 790-784

Received: February 28, 2002; In Final Form: May 21, 2002

Unimolecular dissociations of *o*-, *m*-, and *p*-iodotoluene radical cations that yield $C_7H_7^+$ by loss of an iodine atom have been studied by time-resolved photodissociation (TRPD) spectroscopy using Fourier transform-ion cyclotron resonance mass spectrometry. Iodotoluene radical cations were prepared by the phoionization charge-transfer (PICT) method. The TRPD spectra were obtained in the wavelength range 480−575 nm. The rate-energy data from the present work are combined with the previous rate data obtained in a higher internal energy range to extract activation parameters for unimolecular dissociations. For the direct C−I cleavage channel that leads to tolyl cations, the entropy changes for activation are assumed to be identical to that of the vinylic C−I cleavage of the iodobenzene radical cation, and activation barriers are estimated from thermochemical thresholds. For the lowest barrier rearrangement channel that leads to the benzyl cation, the entropy changes are assumed to be identical to those of the corresponding bromotoluene radical cations. Activation barriers for the rearrangement channel are determined to be 1.77, 1.88, and 1.90 eV for o, m, and p isomers, respectively. Both the product structures and activation parameters for the lowest barrier rearrangement process lend support to the McLafferty mechanism that invokes the H-atom migration from the α to the ipso- or ortho-carbon site and the subsequent H-atom and/or CH_2-group migration on the ring to form benzyl precursors. The effects of halogen substitution (X = Cl, Br, and I) on the rearrangement process are discussed.

I. Introduction

Halotoluene radical cations (X = Cl, Br, and I) with a few eV internal energy dissociate to the $C_7H_7^+$ ions by loss of a halogen atom.[1−18] There are two competing pathways as shown in Figure 1 following Dunbar's notation:[13] the direct C−X cleavage channel I that produces the tolyl cation[2,3,8,18] and the rearrangement channel II that yields the benzyl cation.[15−17] The benzyl structure was identified as the channel II product by product-resolved photodissociations of bromo- and iodotoluene radical cations using Fourier transform ion cyclotron resonance (FT-ICR) spectrometry in our laboratory.[15−17] The lowest barrier product was shown to be the benzyl cation by sustained off-resonance irradiation (SORI) of the *meta*-bromotoluene radical cation using FT-ICR spectrometry.[19]

These two competing pathways have been studied by a number of techniques to determine activation barriers and to assess the tightness of the transition states. Olesik et al.[8] performed photoelectron-photoion coincidence (PEPICO) experiments to obtain the rates of energy-selective dissociations of halotoluene radical cations (Cl, Br, and I) in the internal energy range 2.4−3.8 eV. Dunbar and Lifshitz[9] employed time-resolved photodissociation (TRPD) spectroscopy to measure the rates of one-photon dissociation (1PD) of the *p*-iodotoluene radical cation in the internal energy range 2.17−2.54 eV. Lin and Dunbar[13] measured the 1PD rates of iodotoluene radical cations at the two values of internal energy (2.54 and 2.67 eV) using TRPD spectroscopy. Recently, Cho et al.[14] utilized mass-analyzed ion kinetic energy spectrometry (MIKES) to extract the rates of photodissociation of the *m*-iodotoluene radical cation in the internal energy range 3.7−4.3 eV. More recently, Kim and Shin[16] measured the 1PD rates of bromotoluene radical cations in the internal energy range 2.2−2.7 eV by TRPD spectroscopy. Most recently, Shin et al.[17] reported time- and product-resolved photodissociations of iodotoluene radical cations at 532 and 640 nm.

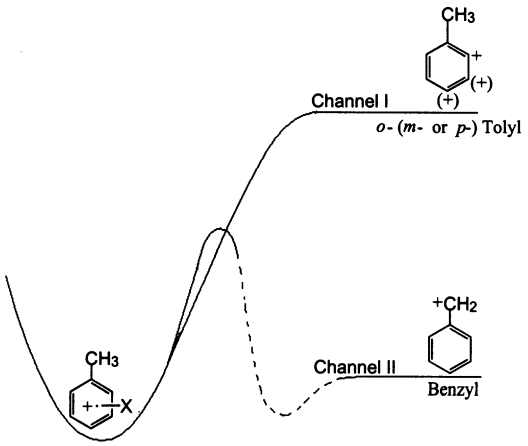

Figure 1. Schematic diagram of the two-channel picture for unimolecular dissociations of halotoluene radical cations.

The rate-energy data were typically fitted to the Rice−Ramsperger−Kassel−Marcus (RRKM) model to extract activation barriers (E_0) and the entropy changes for activation [$\Delta S^{\ddagger}$(1000 K)].[8,20] For chlorotoluenes, the PEPICO data in the

† Part of the special issue "Jack Beauchamp Festschrift".
* To whom correspondence should be addressed.
‡ Korea Research Institute of Standards and Science.
§ Pohang University of Science and Technology.

10.1021/jp025703c CCC: $22.00
Published on Web 07/09/2002

internal energy range 2.4−3.4 eV were enough for the derivation of activation parameters for the lowest activation channel II: $E_0^{II} = 1.70$ eV and $\Delta S^{\ddagger}_{II} = -5.7$ eu for ortho and $E_0^{II} = 1.77$ eV and $\Delta S^{\ddagger}_{II} = -5.7$ eu for both meta- and para isomers.[8] For bromotoluenes, Kim and Shin[16] combined their TRPD data in the internal energy range 2.2−2.7 eV with the complementary PEPICO data in the internal energy range 2.7−3.5 eV to derive $E_0^{II} = 1.66$ eV and $\Delta S^{\ddagger}_{II} = -9.0$ eu for ortho, $E_0^{II} = 1.80$ eV and $\Delta S^{\ddagger}_{II} = -7.2$ eu for meta, and $E_0^{II} = 1.78$ eV and $\Delta S^{\ddagger}_{II} = -5.6$ eu for para isomers. For iodotoluenes, Lin and Dunbar[13] combined their TRPD data with the PEPICO results for *p*-iodotoluene to derive activation parameters that were identical for all three isomers: $E_0^{II} = 1.88$ eV and $\Delta S^{\ddagger}_{II} = -7.0$ eu. No differentiation among the three isomers was made partly due to a limited number of the rate-energy data. Unlike chloro- and bromotoluenes, activation barriers of the two competing channels in iodotoluenes are so close to each other that the data analysis using the RRKM model is complicated.[13] To differentiate activation parameters among the three isomers and to help establish the mechanism of the rearrangement process, more kinetic data are needed in a wider internal energy range.

In the present study, time-resolved photodissociations of iodotoluene radical cations were studied in the internal energy range 2.2−2.7 eV using FT-ICR spectrometry. To prepare the parent ions under a well-defined internal energy condition and to reduce the uncertainty in ion temperature, the parent ions were produced by the photoionization-charge-transfer (PICT) method.[15] The parent ions were then optically excited to the upper electronic state in the wavelength range 480−575 nm.[21] The rapid internal conversion to the ground electronic state prepares vibrationally hot parent ions. Rates of 1PD of iodotoluene radical cations were measured by TRPD spectroscopy.[9,13,15−17,22−25] The TRPD rate measurements at higher internal energies were limited by the falloff of the optical absorption cross section of iodotoluene radical cations[21] and by the experimental time resolution set by the ICR excitation pulse width. The present TRPD data were combined with other complementary kinetic data available at higher internal energies for the refinement of RRKM parameters. In light of activation parameters for the lowest barrier rearrangement processes in halotoluene (Cl, Br, and I) radical cations, the rearrangement mechanism is elucidated, and the effects of halogen subsitution on the sigmatropic rearrangement process are discussed.

II. Experimental Section

FT-ICR experimental setups for TRPD spectroscopy were previously described in detail.[15] The FT-ICR spectrometer consists of a 5.0 T superconducting magnet (Oxford), a home-built vacuum chamber with a 2 in. cubic trapping ICR cell, and an IonSpec Omega/486 FT-data system. There were 0.325 in. holes in the centers of both trapping plates to provide optical access along the axial direction. The background pressure in the ICR chamber was typically below 9×10^{-10} Torr.

All chemicals were purchased from Aldrich Inc. and used without further purification after several freeze−pump−thaw cycles. Gaseous iodotoluenes and toluene-d_8 were separately guided into the ICR cell by two electropolished stainless steel tubes connected to either a leak valve or a pulsed valve. The purity of each sample was tested by EI mass spectra. Sample inlet lines were baked and pumped out overnight to prevent any cross-contamination between isomers. EI mass spectra of residual background in both the ICR chamber and the inlet lines were checked before introducing a new sample. Partial pressures of iodotoluenes and toluene-d_8 were kept constant at 4×10^{-8} and 2×10^{-8} Torr, respectively.

The PICT involves a sequence of ionization and charge-transfer processes 1−3:

$$C_6D_5CD_3 + 2h\nu\ (266\ \text{nm}) \rightarrow C_6D_5CD_3^{+\bullet} + e^- \quad (1)$$

$$C_6D_5CD_3^{+\bullet} + CH_3C_6H_4I \rightarrow C_6D_5CD_3 + CH_3C_6H_4I^{+\bullet} \quad (2)$$

$$CH_3C_6H_4I^{+\bullet} + CH_3C_6H_4\mathbf{I} \rightarrow CH_3C_6H_4I + CH_3C_6H_4\mathbf{I}^{+\bullet} \quad (3)$$

Two-photon ionization (2PI) of toluene-d_8 at 266 nm yielded its radical cation. Because the ionization potential (IP) of toluene-d_8, 8.8276 eV,[26] is higher than IPs of iodotoluenes, 8.44−8.58 eV,[8] toluene-d_8 radical cations undergo the charge-transfer process in eq 2 with iodotoluenes to produce the parent ions. Vibrationally hot iodotoluene radical cations were then thermalized by both radiative relaxation and thermoneutral charge-exchange collisions with the parent neutrals at room temperature.[15] Unlike electron impact (EI) ionization, the PICT in the absence of resistive heating of the ICR cell by hot filament ensures a thermal internal energy distribution of the parent ion.[15]

The 266 nm output of a Q-switched Nd:YAG laser (Spectra-Physics, GCR-150) was used for 2PI of toluene-d_8. A 3 mm diameter laser beam was used unfocused with a laser power of 1−3 mJ/pulse. Photolyses of iodotoluene radical cations were achieved in the wavelength range 480−575 nm by a counter-propagating second laser beam that overlapped with the ionization laser beam. The wavelength range 500−550 nm was covered by a dye laser (Continuum, ND-6000) with Coumarine-500 pumped by the 355 nm output of a Q-switched Nd:YAG laser (Continuum, NY-8010). The shorter wavelength range 480−500 nm was provided by the same dye laser with Coumarine-480. The wavelength longer than 550 nm was generated by the same dye laser with Rhodamine-590 pumped by the 532 nm output of the Q-switched Nd:YAG laser. The photolysis laser beam was adjusted to a 2 mm diameter at a typical laser power of 1−3 mJ/pulse.

The photolysis laser was delayed 2s after two-photon ionization of toluene-d_8. It allows the charge-transfer reaction of toluene-d_8 radical cations with idotoluenes and the subsequent charge-exchange thermalization. Because there is no resistive heating of the ICR cell by a hot filament, the temperature of the molecules is considered to be the same as the vacuum housing temperature (293 K).[15] For the time-resolved observation of photodissociation processes, the temporal buildup of $C_7H_7^+$ was monitored as a function of time delay between the photolysis laser and the beginning of the radio frequency (rf) detection pulse of 20 μs duration. The detection rf was on resonance with the ICR frequency of $C_7H_7^+$. A precise timing of the photodissociation laser pulse was monitored by a fast photodiode using a digital oscilloscope (Lecroy 9304AM).

III. Results

A. Time-Resolved Photodissociation (TRPD) Spectra. TRPD spectra of *o*-, *m*-, and *p*-iodotoluene radical cations are shown in Figures 2−4, respectively. All three isomers exhibited nonzero ion signals at $t = 0$ owing to multiphoton processes as reported previously.[16,17] Multiphoton products appeared within the rf excitation pulse duration of 20 μs. The relative intensity of the time-zero intercept increased as the laser power increased, confirming that the initial fast rising components resulted from multiphoton processes. Hence, the laser power was adjusted in such a way to make the one-photon process become dominant. Because the multiphoton product signals appear within the first

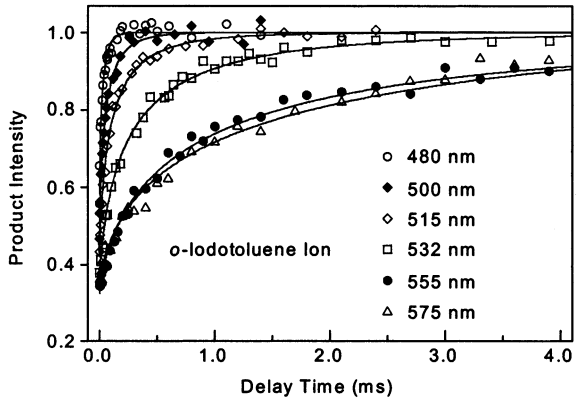

Figure 2. TRPD spectra of the *o*-iodotoluene radical cation at 575, 555, 532, 515, 500, and 480 nm. The solid curves are the calculated TRPD spectra using the convoluted signal equation with the RRKM parameters reported in Table 3.

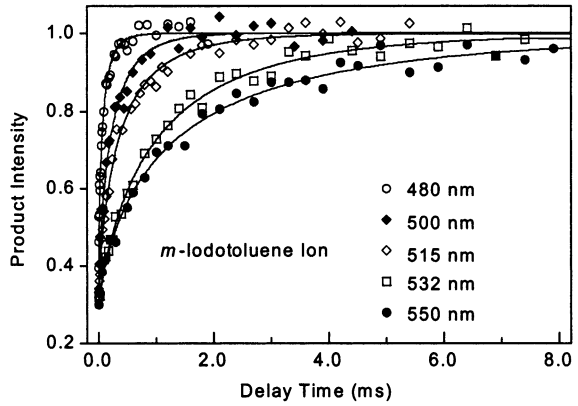

Figure 3. TRPD spectra of the *m*-iodotoluene radical cation at 550, 532, 515, 500, and 480 nm with the best fit curves using the convoluted signal equation with the RRKM parameters reported in Table 3.

20 μs to give an intercept,[17] the slow rising signal results from the single-photon dissociation only. The unimolecular dissociation rate is extracted from the slow rising component.

To extract the rate constant, TRPD spectra were fitted to the ICR-signal equation convoluted with a truncated Boltzmann distribution of the parent ion at room temperature.[15,16,22,27−30] The TRPD ICR signal equations are given in eqs 4 and 5:[30]

$$S(t) = C(t + \Delta - t_0)\left\{1 - \frac{1 - \exp[-k(t + \Delta - t_0)]}{k(t + \Delta - t_0)}\right\} \quad \text{for } t_0 - \Delta \le t \le t_0 \quad (4)$$

$$S(t) = C\Delta\left\{1 - \exp[-k(t - t_0)]\frac{1 - \exp(-k\Delta)}{k\Delta}\right\} \quad \text{for } t_0 \le t \quad (5)$$

where $S(t)$ is the product ion signal, C is the proportionality constant, Δ is the width of the single rf burst, and k is the dissociation rate constant. The probe laser was fixed at t_0 while the detection rf burst was scanned. Equations 4 and 5 correspond to a timing that the rf excitation begins before and after the probe laser. The parent ion correction terms are neglected because the dephasing rate in a 5 T magnetic field is much faster than the dissociation rate.[30]

Because the rate constant k is a function of the internal energy, $k(h\nu + E)$, where E is the internal energy of the parent ion, the signal equation is convoluted with an internal energy distribution

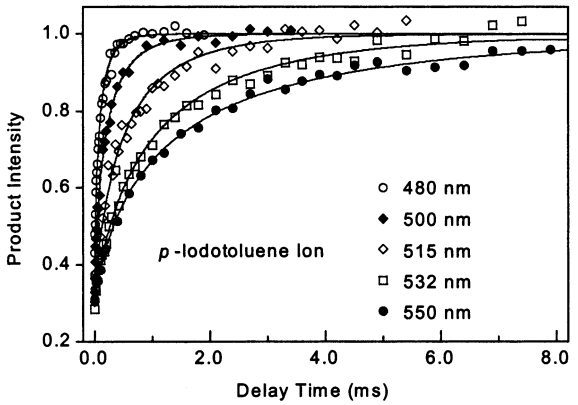

Figure 4. TRPD spectra of the *p*-iodotoluene radical cation at 550, 532, 515, 500, and 480 nm with the best fit curves using the convoluted signal equation with the RRKM parameters reported in Table 3.

of the parent ion at a given initial temperature as given in eq 6:[29]

$$\langle S(t)\rangle = \sum_{E=0}^{E_0} P(E)S(t) \quad (6)$$

where $S(t)$ is the convoluted signal equation, E_0 is the lowest dissociation threshold, and $P(E)$ is the probability of having a vibrational energy E at a given initial temperature. Because the parent ion population is depleted above E_0 due to dissociation, $P(E)$ is calculated using a truncated Boltzmann distribution as given in eqs 7 and 8:[27,28]

$$P(E) = \frac{\rho(E)\exp(-E/kT)}{Q} \quad (7)$$

$$Q = \sum_{E=0}^{E_0} \rho(E)\exp(-E/kT) \quad (8)$$

where $\rho(E)$ is the density of states of molecule and Q is the vibrational partition function. $\rho(E)$ is obtained by directly counting the number of states in harmonic oscillators. Vibrational frequencies are taken from ref 8. Thus, the convoluted ICR-signal equation considers both the thermal internal energy distribution of the parent ions and the energy dependence of the rates.

The average rate constants are derived from the TRPD data range from 6×10^2 to 6×10^4 s^{-1}. As the rate of photodissociation decreases, the rate of infrared radiative relaxation that depletes the parent ion populated above the activation barrier becomes increasingly important.[9] At the longest wavelengths, the apparent rate constants were only a few times greater than the IR relaxation rate of 160 s^{-1} reported for the *p*-iodotoluene radical cation.[9] To account for the IR relaxation rate, the value of 160 s^{-1} was assumed for all three isomers at all wavelengths. RRKM activation parameters were refined until the calculated TRPD curves best fit experiments at all wavelengths. The solid lines drawn in Figures 2−4 represent the final best-fit curves.

The average dissociation rate constants are summarized in Table 1 and plotted as a function of internal energy in Figures 5−7 for *o*-, *m*-, and *p*-iodotoluene radical cations, respectively. The present results are depicted as solid symbols, whereas the rates from other workers[8,10,13,14] are shown as open symbols. Open triangles in Figures 5−7 represent the rate constants at 532 and 504 nm, reported by Lin and Dunbar using TRPD

TABLE 1: Rate Constants of One-Photon Dissociation of Iodotoluene Radical Cations[a]

wavelength (nm)	$\langle E_{th}\rangle + h\nu$ (eV)	k (s^{-1})[b] ortho	meta	para
575	2.263	660 ± 130		
555	2.341	1190 ± 100		
550	2.361		600 ± 100	560 ± 50
532[c]	2.436	4300 ± 300	890 ± 60	850 ± 100
515	2.514	13000 ± 1200	2740 ± 150	1940 ± 130
500	2.586	24100 ± 2000	4500 ± 400	4840 ± 240
480	2.690	54800 ± 7000	14600 ± 1300	10800 ± 1000

[a] Rate constants were corrected for the IR relaxation rate of 160 s^{-1} (ref 9). [b] Errors are estimated from the uncertainty of fitting TRPD spectra. [c] Reference 17.

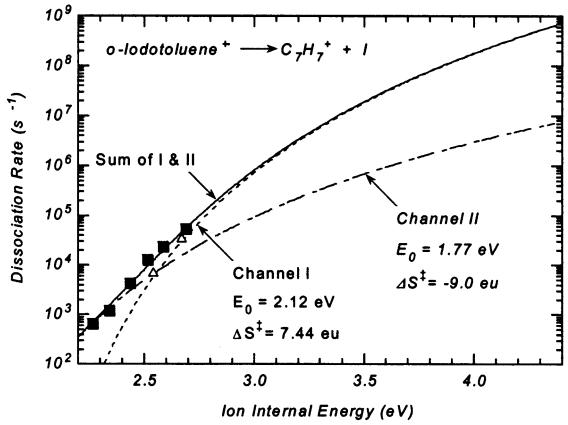

Figure 5. RRKM rate-energy curves for the *o*-iodotoluene radical cation. Solid squares represent the data from the present work and open triangles from Lin and Dunbar's works (ref 13). The solid line is the sum of channels I and II. Activation parameters are listed in Table 3.

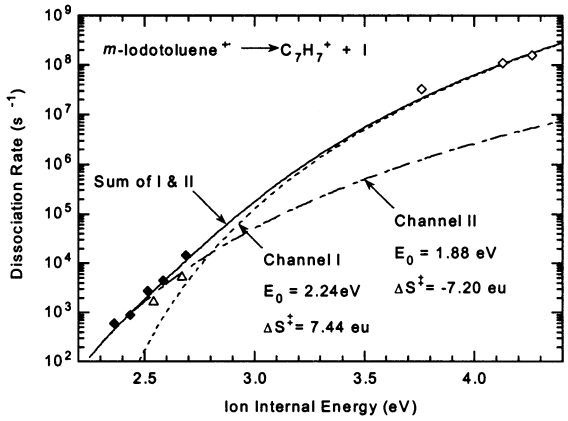

Figure 6. RRKM rate-energy curves for the *m*-iodotoluene radical cation. Solid diamonds represent the data from the present work, open diamonds represent the data from Cho et al.'s PD-MIKES studies (ref 14), and open triangles represent the data from Lin and Dunbar's works (ref 13).

spectroscopy.[13] Open diamonds in Figure 6 denote the rate constants of the *m*-iodotoluene radical cation measured by Kim and co-workers[10,14] using MIKES in the internal energy range 3.7−4.3 eV. Open circles in Figure 7 are from Olesik et al.'s PEPICO experiment[8] on the *p*-iodotoluene radical cation in the internal energy range 2.9−3.8 eV. For the o isomer, no rate-energy data were available in a higher internal energy range. The PEPICO data for the p isomer need a few comments. Olesik et al.[8] originally analyzed their PEPICO spectra with biexponential decay functions. Their spectra were later reanalyzed by Lin and Dunbar assuming a single-exponential decay. The rate constants adopted in Figure 7 were taken from Lin and Dunbar's

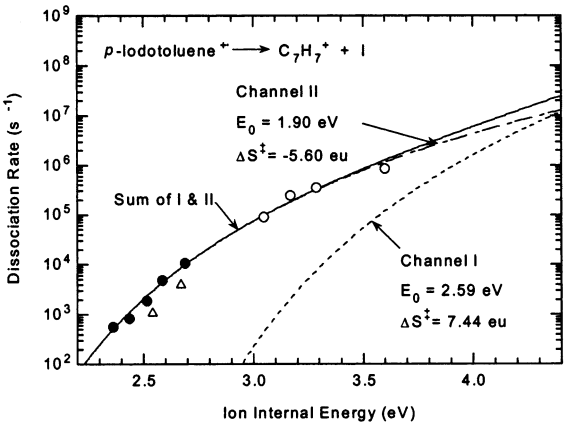

Figure 7. RRKM rate-energy curves for the *p*-iodoluene radical cation. Solid circles represent the data from the present work, open circles represent the data from Olesik et al.'s PEPICO studies (ref 8), and open triangles represent the data from Lin and Dunbar's works (ref 13).

analysis,[13] but the average internal energy of the ion was taken from the original work.[8] We noted that the ion internal energy of each PEPICO data point used by Lin and Dunbar was slightly higher than the original report. After close inspection, we decided to adopt values of internal energy from the original work that considered the thermal energy of neutrals at 298 K rather than those considered by Lin and Dunbar.

The present experiments at 532 and 500 nm resulted in 1PD rates of all three isomers slightly slower than those of Lin and Dunbar's at 532 and 504 nm, respectively, due to a lower ion temperature in our study. When the thermal energy is taken into account, Lin and Dunbar's rates are slightly less than ours. Both studies employ the same TRPD methodology, but they differ in preparation of iodotoluene radical cations. EI was used by Lin and Dunbar, whereas PICT was used in this work. In both experiments, the parent ions were thermalized by radiative relaxation and charge-exchange collisions with the parent neutrals. With PICT, the ion temperature is well defined to the vacuum housing temperature of 293 K, as there is no resistive heating of the ICR cell by a hot filament. On the other hand, with EI, the ion temperature is uncertain as it varies with the filament current, the duration of resistive heating, and the efficiency of heat dissipation by surroundings.[15] Comparisons of the present results with those of Lin and Dunbar indicate that the ion temperature in Lin and Dunbar's work may be lower than their assigned temperature 375 K.

B. Kinetic Modeling and RRKM Parameters. The microcanonical RRKM rate constant at the internal energy E is given by eq 9:[8,20]

$$k(E) = \frac{\sigma W^{\ddagger}(E - E_0)}{h\rho(E)} \tag{9}$$

where σ is the reaction degeneracy, E and E_0 are the ion internal energy and the activation barrier, respectively, $W^{\ddagger}(E - E_0)$ is the sum of internal energy states in the transition state from 0 to $E - E_0$, and $\rho(E)$ is the density of states of the parent ion at energy E. The molecular parameters required for evaluation of the rates are the vibrational frequencies of the transition state and the parent ion and the activation barrier, E_0. The vibrational frequencies of the parent ions and transition states are taken from ref 8. The transition-state frequencies are treated as adjustable parameters. The character of the transition state is then expressed by the activation entropy, $\Delta S^{\ddagger}$, as determined

TABLE 2: Thermochemical Data for Chemical Species Related to This Work

M	IP(M) (eV)	$\Delta H_f^o{}_0(M^+)$ (kJ mol^{-1})
o-$CH_3C_6H_4I$	8.58 ± 0.01[a]	984 ± 6[a]
m-$CH_3C_6H_4I$	8.56 ± 0.01[a]	982 ± 6[a]
p-$CH_3C_6H_4I$	8.43 ± 0.01[a]	958 ± 6[a]
$C_6D_5CD_3$ (toluene-d_8)	8.8276 ± 0.0006[b]	924[e]
$C_6H_5CH_2$ (benzyl)	7.2489 ± 0.0006[c]	919 ± 5[f,g]
c−C_7H_7 (tropylium)	6.221 ± 0.006[d]	896 ± 8[g]
o- $C_6H_4CH_3$ (*o*-tolyl)		1087 ± 8[g]
m- $C_6H_4CH_3$ (*m*-tolyl)		1093 ± 8[g]
p- $C_6H_4CH_3$ (*p*-tolyl)		1101 ± 8[g]
$\Delta H_f{}_0{}_0(I)$[a]= 107.2 kJ mol^{-1}		

[a] Reference 8. [b] Reference 26. [c] Reference 31. [d] Reference 32. [e] Reference 33. [f] Reference 18. [g] Reference 34.

from the canonical partition functions:[8,20]

$$\Delta S^{\ddagger} = k_B \ln \frac{\prod q_i^{\ddagger}}{\prod q_i} + \frac{U^{\ddagger} - U}{T} \qquad (10)$$

where q is the vibrational partition function and $U^{\ddagger}$ and U are the average vibrational energies at temperature T. The activation entropy is evaluated at 1000 K to be consistent with others.[8,20]

Although there are a number of variables involved in the RRKM rates, there are only two independent parameters: the activation barrier, E_0, and the activation entropy, $S^{\ddagger}$. Thus, for each iodotoluene radical cation isomer, there are four parameters to fit the rate constants using the RRKM model: E_0^{I} and $\Delta S^{\ddagger}_{I}$ for channel I and E_0^{II} and $\Delta S^{\ddagger}_{II}$ for channel II.

To determine kinetic parameters, the present results were combined with the complementary data available at higher internal energies. Although the present study provides more rate-energy data for each isomer, it is not feasible to determine all four kinetic parameters independently. Our TRPD data span the internal energy range near thresholds for channel II, so that they are more reliable for the derivation of the channel II kinetic parameters. For the channel I kinetic parameters, both the channel branching ratios and the dissociation rates need to be measured in an internal energy range where the contributions from both channels are comparable to each other. The number of independent variables was reduced by fixing activation parameters for channel I to those available from the previous studies of tolyl, iodotoluene, and iodobenzene radical cations. In addition, the entropy changes for activation in channel II were fixed to those of the corresponding bromotoluene radical cations.[16]

For channel I, it was assumed that the direct C−I cleavage proceeded via a loose transition state similar to that of the iodobenzene radical cation and that the effect of the methyl substitution in place of hydrogen atom was negligible on the entropy change. Moreover, the loose transition state was assumed to be product-like with no reverse barrier. The $\Delta S^{\ddagger}_{I}$ value of 7.44 eu was taken from the vinylic C−I cleavage of the iodobenzene radical cation as suggested by Lin and Dunbar.[13] Activation barriers for channel I were initially assumed to be identical to thermochemical thresholds, and then they were adjusted later to fit the available experimental rate-energy data. Thermochemical data for iodotoluenes, tolyl cations, and iodine atom are listed in Table 2 along with those for toluene, benzyl, and tropylium radicals and cations.[31−33] Heats of formation of tolyl cations were taken from the values recommended by Shin from ab initio calculations.[34] Thermochemical thresholds for channel I are estimated to be 2.18 ± 0.1, 2.26 ± 0.1, and 2.59 ± 0.1 eV for *o*-, *m*-, and *p*-iodotoluene radical cations, respectively.[34]

TABLE 3: RRKM Kinetic Parameters E_0 and $\Delta S^{\ddagger}$(1000 K) for Iodotoluene Radical Cations

	ortho	meta	para		ortho	meta	para
	(a) Channel I				(b) Channel II		
E_0^{I}(eV)	2.12[a]	2.24[a]	2.59[b]	E_0^{II}(eV)	1.77[c]	1.88[c]	1.90[c]
$\Delta S^{\ddagger}_{I}$(eu)	7.44	7.44	7.44	$\Delta S^{\ddagger}_{II}$(eu)	−9.00	−7.20	−5.60

[a] Estimated errors are 0.04 eV. [b] Assumed to be identical to the calculated thermochemical threshold (ref 34). [c] Estimated errors are 0.02 eV.

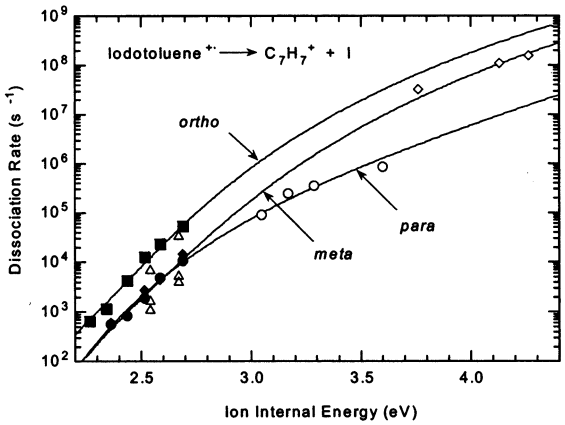

Figure 8. RRKM rate-energy curves for all three isomers (sum of channels I and II).

For channel II, the $\Delta S^{\ddagger}_{II}$ values taken from bromotoluene radical cations are −9.0, −7.2, and −5.6 eu for ortho, meta, and para isomers, respectively.[16]

For both o and m isomers, activation barriers for channel I are quite low so that channel I competes with channel II in the internal energy range 2.2−2.7 eV. Therefore, both E_0^{I} and E_0^{II} were adjusted to fit the experimental data to the sum of the calculated rates for both channels. Adopting $\Delta S^{\ddagger}_{I}$ values from that of the iodobenzene radical cation and $\Delta S^{\ddagger}_{II}$ values from those of bromotoluene radical cations yielded E_0^{I} = 2.12 eV and E_0^{II} = 1.77 eV for ortho and E_0^{I} = 2.24 eV and E_0^{II} = 1.88 eV for meta. The activation barrier for channel I of the ortho isomer decreases slightly from the initially assigned value of 2.18−2.12 eV, but it still lies within the uncertainty of the calculated thermochemical threshold of 2.18 eV ± 0.1 eV. For meta, the value of E_0^{I} = 2.24 eV is in close agreement with the thermochemical threshold of 2.26 ± 0.1 eV. The best fit curves are shown in Figures 5 and 6 along with the measured rate constants. The para isomer is the least complicated system among three isomers because the channel I threshold is much higher than that of channel II. The rates for channel I with E_0^{I} = 2.59 eV and $\Delta S^{\ddagger}_{I}$ = 7.44 eu are several orders of magnitude less than the rates for channel II in the internal energy range 2.2−3.8 eV as shown in Figure 7. Hence, the previous PEPICO data and the present TRPD results were combined to extract the RRKM kinetic parameters for channel II only. Adopting $\Delta S^{\ddagger}_{II}$ = −5.6 eu fitted experiments very well and yielded E_0^{II} = 1.90 eV. The refined RRKM parameters are listed in Table 3.

The rate-energy curves for all three isomeric ions are plotted in Figure 8 for direct comparisons. The slopes are different mostly due to the entropy changes in channel II. Activation barriers for channel II are in ascending order of ortho < meta ≤ para, which is similar to the ordering observed in chloro- and bromotoluene radical cations.[8,16] Yields of channel I and II

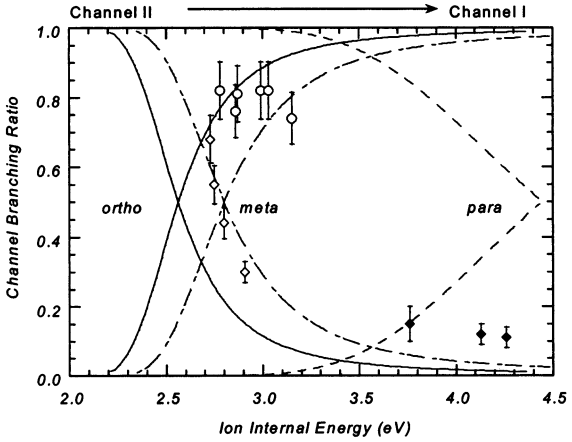

Figure 9. Yields of channels I and II as a function of internal energy of iodotoluene radical cations. Open symbols are taken from Lifshitz et al. (ref 11), and solid diamonds are taken from Cho et al. (ref 14).

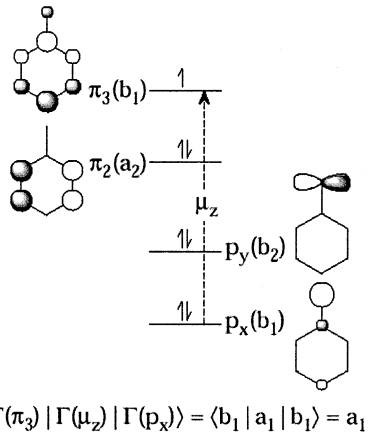

Figure 10. Schematic diagram of the highest lying occupied molecular orbitals of halobenzene radical cations.

are calculated from the refined RRKM parameters for all three isomers, and they are shown in Figure 9 as a function of internal energy. Channel II is dominant in the low internal energy range, whereas channel I becomes increasingly important as the internal energy increases. Open circles represent the channel-II yields from the para isomer reported by Lifshitz et al.,[11] open diamonds correspond to the channel-II yields from the meta isomer reported by Lifshitz et al.,[11] and solid diamonds denote the channel-II yields from the meta isomer reported by Cho et al.[14] The general trends observed in experiments are well reproduced by the present kinetic model, but they differ in details. The apparent discrepancy is most likely due to the wide internal energy distribution of iodotoluene radical cations prepared by either EI or chemical ionization (CI). Lifshitz et al. prepared the m and p isomers by EI in an ion trap and analyzed metastable peak shapes in the internal energy range 2.7−3.1 eV. Cho et al. prepared the m isomer by CI and derived the branching ratios from the MIKES line shape analysis. Further investigations are recommended for the precise measurement of the channel branching ratios from energy-selective dissociations of iodotoluene radical cations in the internal energy range where the predicted branching ratios are about 0.3−0.7.

IV. Discussion

Photodissociations of iodotoluene radical cations in the wavelength range 480−575 nm are known to occur via the $\pi \leftarrow n$ electronic transition that involves the halogen-to-ring charge transfer.[21,35] Photoelectron spectra of halotoluenes are quite similar to those of the corresponding halobenzenes.[36,37] In photoelectron spectra of halobenzenes (X = Cl, Br, and I), the 2-fold degeneracy of e_{1g} orbitals of the benzene radical cation is removed by the presence of halogens.[37] At the point of substitution, one of the orbitals (b_1-type) has its maximum electron-density, whereas the other (a_2-type) has a node as shown in Figure 10. The resonance effect of halogen allows the donation of electron density of lone-pair orbitals to the benzene ring, affecting the b_1-type π_3 orbital. Thus, in photoelectron spectra of halotoluenes, the lowest-energy ionization band has a hole in the b_1-type π_3 orbital. The dipole-allowed optical transition involves the charge transfer from an out-of-plane (b_1-type) p_x orbital of the I atom to the b_1-type π_3 orbital of the ring with the transition dipole moment aligned along the C−I bond axis [$\langle G(\pi_3)|\Gamma(\mu_z)|\Gamma(p_x)\rangle = \langle b_1|a_1|b_1\rangle = a_1$].

The photoexcited parent radical cations undergo rapid internal conversion to the ground electronic state as is evident from the absence of fluorescence from the excited parent ions.[38] The strong state mixing by resonance between the b_1-type p_x orbital of iodine and the b_1-type π_3 orbital of the ring also helps promoting internal conversion processes between the same symmetry states. In the internal energy range 2.2−2.7 eV, the intramolecular vibrational energy redistribution (IVR) is considered to be very fast compared with the rates of dissociation on the order of 10^3-10^5 s^{-1} and the rate of IR radiative relaxation of 160 s^{-1}. Rapid IVR allows the molecule to populate all of the statistical phase space throughout its dissociation so that the RRKM model is properly justified.[20]

One of the most intriguing results is that adopting the $\Delta S^{\ddagger}_{II}$ value of −5.6 eu from *p*-bromotoluene[16] reproduces the rate-energy curve for *p*-iodotoluene very well in the wide internal energy range 2.2−3.8 eV. This value is almost identical to the $\Delta S^{\ddagger}_{II}$ value of −5.7 eu obtained for *p*-chlorotoluene.[8] Adopting the $\Delta S^{\ddagger}_{II}$ values of −9.0 and −7.2 eu from the *o*- and *m*-bromotoluene radical cations, respectively, also works well for the corresponding iodotoluene radical cations with only minor adjustments in E_0^{I} for both ortho and meta isomers. These results suggest that the halogen atom itself is not an active species migrating in the rearrangement process but its position on the ring influences the intramolecular dynamics of the rearrangement process.

Activation barriers for channel II (E_0^{II}) are determined to be 1.77, 1.88, and 1.90 eV for *ortho*, *meta*, and *para*-iodotoluene radical cations, respectively. In comparison, E_0^{II} in chlorotoluenes[8] were reported to be 1.70, 1.77, and 1.77 eV, and E_0^{II} in bromotoluenes[16] were 1.66, 1.80, and 1.78 eV for o, m, and p isomers, respectively. Because the C−X cleavage is not the rate-limiting step, activation barriers for channel II are not strongly affected by the halogen substitution. The slight increase in activation barrier in going from chlorine to iodine may be related to the resonance effect of halogen. IPs of halotoluenes decrease from ∼8.8 to ∼8.5 eV in going from chlorine to iodine,[8] indicating that the interaction between the highest lying occupied π_3 orbitals of the ring and that the p_x lone-pair orbital of halogen becomes more repulsive in going from chlorine to iodine. Thus, in halotoluene radical cations, the resonance interaction makes the iodine atom carry more partial positive charge than chlorine or bromine. Consequently, the ring carbons in the iodotoluene radical cation carry less positive charge character than those in the chloro- or bromotoluene radical cation. It is well-known that the positive charge character on the empty carbon site helps the H-atom migration by forming nonclassical three-center two-electron bonds in the transition state.[39] A π_3-p_x resonance interaction in iodotoluene radical cation disfavors the formation

of the transition state for the H-atom migration. In addition, for all three halotoluenes, the ortho isomers possess the lowest activation barriers. This ortho effect may be related to the extent of the polarization of the methyl-to-ring C−C bond induced by the adjacent ortho polar C−X bond.[40] A more positive charge is localized on the ipso or ortho carbon by the ortho halogen than by the meta or para halogen, thereby better stabilizing the transition state for the α H-atom migration.

The structure of $C_7H_7^+$ from channel II also provides valuable information about the rearrangement mechanism. It has been supposed for a long time that the rearrangement mechanism of halotoluene radical cations is similar to that of the toluene radical cation that involves the ring expansion to the cycloheptatriene radical cation.[1,2,4,8,10,11,13,14,41] The ring-expansion mechanism was purported by the evidence from collisional activation (CA) studies by McLafferty et al.[3] and Olesik et al.,[8] who suggested the formation of the tropylium cation from channel II. However, the energy-selective studies in our laboratory clearly show that channel II leads predominantly to the benzyl cation from both bromo- and iodotoluene radical cations.[16,17] The sustained off-resonance irradiation (SORI) experiments substantiate this conclusion.[19] Furthermore, our study of time- and product-resolved photodissociations of iodotoluene radical cations at 532 and 640 nm has revealed that the tropylium ion derives from the isomerization of tolyl cations produced from channel I.[17]

The mechanism of the benzyl cation formation from channel II may be similar to the McLafferty mechanism proposed for bromotoluene radical cations in our previous paper.[16] This mechanism invokes the migration of an α H atom to the benzene ring by either [1,2] α-H migration or [1,3] α-H migration or both that leads to the isomerization of halotoluene radical cations to the precursors for the benzyl cation. The absence of the tropylium cation from channel II indicates that the ring expansion to form the cycloheptatrienyl halide radical cation is kinetically less favored than the formation of benzyl precursors. There are two possible precursors: methylene cyclohexadienyl halide and benzyl halide. The formation of the former species involves the H-atom migration on the ring, whereas that of the latter species involves the migratory insertion of methylene into the C−X bond.

V. Conclusion

In a series of TRPD studies using FT-ICR spectrometry, we provided a wealth of information about the kinetics of the lowest barrier rearrangement processes in bromo- and iodotoluene radical cations. Unlike the toluene radical cation that yields the tropylium ion as the lowest barrier fragment, the halogen substitution (X = Cl, Br, and I) in place of the ring hydrogen resulted in the benzyl cation as the lowest barrier product. Almost identical activation barriers among three halogenated species suggest that the C−X bond cleavage is not the rate-determining step in rearrangement. The rate-determining step involves the H-atom migration from the α- to the ipso or ortho carbon or the subsequent migrations of either the H atom or CH_2 group along the benzene ring or both. The entropy changes for rearrangement are determined by the dynamics of the H-atom and/or CH_2-migration processes. The present result establishes the lowest activation pathway in halotoluene radical cations and calls for the investigation of the similar processes in the toluene radical cation.[41]

Acknowledgment. S.K.S. acknowledges the partial support from the National Science Foundation Young Investigator Award (CHE-9457668) while at the University of California, Santa Barbara, the National Research Laboratory Program of Korea Institute of Science and Technology Evaluation and Planning, and the Brain Korea 21 Program.

References and Notes

(1) Yeo, A. N. H.; Williams, D. H. *Chem. Commun*. **1970**, 886.

(2) Winkler, J.; McLafferty, F. W. *J. Am. Chem. Soc.* **1973**, *95*, 7533.

(3) McLafferty, F. W.; Winkler, J. *J. Am. Chem. Soc*. **1974**, *96*, 5182.

(4) Stapleton, B. J.; Bowen, R. D.; Williams, D. H. *J. Chem. Soc., Perkin Trans. II*, **1979**, 1219.

(5) Proctor, C. J.; McLafferty, F. W. *Org. Mass. Spectrom.* **1983**, *18*, 193.

(6) Dunbar, R. C.; Weddle, G. H. *J. Phys. Chem.* **1988**, *92*, 5706.

(7) Dunbar, R. C.; Honovich, J. P.; Asamoto, B. *J. Phys. Chem.* **1988**, *92*, 6935.

(8) Olesik, S.; Baer, T.; Morrow, J. C.; Ridal, J. J.; Buschek, J.; Holmes, J. L. *Org. Mass Spectrom.* **1989**, *24*, 1008.

(9) Dunbar, R. C.; Lifshitz, C. *J. Chem. Phys*. **1991**, *94*, 3542.

(10) Choe, J. C.; Kim, M. S. *Int. J. Mass Spectrom. Ion Processes* **1991**, *107*, 103.

(11) Lifshitz, C.; Levin, I.; Kababia, S.; Dunbar, R. C. *J. Phys. Chem.* **1991**, *95*, 1667.

(12) Lablanquie, P.; Ohashi, K.; Nishi, N. *J. Chem. Phys*. **1993**, *98*, 399.

(13) Lin, C. Y.; Dunbar, R. C. *J. Phys. Chem.* **1994**, *98*, 8. 1369.

(14) Cho, Y. S.; Kim, M. S.; Choe, J. C. *Int. J. Mass Spectrom. Ion Processes* **1995**, *145*, 187.

(15) Shin, S. K.; Han, S.-J.; Kim, B. *Int. J. Mass Spectrom. Ion Processes* **1996**, *158*, 345.

(16) Kim, B.; Shin, S. K. *J. Chem. Phys.* **1997**, *106*, 1411.

(17) Shin, S. K.; Kim, B. Han, S.-J.; Jarek, R. L. *Bull. Korean Chem. Soc.* **2002**, *23*, 267.

(18) Baer, T.; Morrow, J. C.; Shao, J. D.; Olesik, S. *J. Am. Chem. Soc.* **1988**, *110*, 5633.

(19) Shin, S. K.; Han, S.-J. unpublished.

(20) Baer, T.; Hase, W. L. *Unimolecular Reaction Dynamics: Theory and Experiment*; Oxford: New York, 1996; Chapter 7.

(21) Fu, E.; Dymerski, P. P.; Dunbar, R. C. *J. Am. Chem. Soc*. **1976**, *98*, 337.

(22) Dunbar, R. C. *J. Phys. Chem.* **1987**, *91*, 2801.

(23) Huang, F. S.; Dunbar, R. C. *J. Am. Chem. Soc.* **1990**, *112*, 8167.

(24) Huang, F. S.; Dunbar, R. C. *Int. J. Mass Spectrom. Ion Processes* **1991**, *109*, 151.

(25) Faulk, J. D.; Dunbar, R. C. *J. Phys. Chem*. **1991**, *95*, 6932.

(26) Lu, K. T.; Eiden, G. C.; Weisshaar, J. C. *J. Phys. Chem.* **1992**, *96*, 9742.

(27) Dunbar, R. C. *J. Chem. Phys.* **1991**, *95*, 2537.

(28) Dunbar, R. C. *J. Phys. Chem.* **1994**, *98*, 8705.

(29) Faulk, J. D.; Dunbar, R. C.; Lifshitz, C. *J. Am. Chem. Soc.* **1990**, *112*, 7893.

(30) Dunbar, R. C. *J. Chem. Phys.* **1989**, *91*, 6080.

(31) Eiden, G. C.; Lu, K. T.; Badenhoop, J.; Weinhold, F.; Weisshaar, J. C. *J. Chem. Phys.* **1996**, *104*, 8886.

(32) Johnson, R. D. *J. Chem. Phys*. **1991**, *95*, 7108.

(33) Lias, S. G.; et al. *J. Phys. Chem. Ref. Data* **1988**, *17*, Suppl. 1.

(34) Shin, S. K. *Chem. Phys. Lett.* **1997**, *280*, 260.

(35) Dymerski, P. P.; Fu, E.; Dunbar, R. C. *J. Am. Chem. Soc.* **1974**, *96*, 4109.

(36) Kimura, K.; Katsumata, S.; Achiba, Y.; Yamazaki, T.; Iwata, S. *Handbook of HeI Photoelectron Spectra of Fundamental Organic Molecules*; Japan Scientific Societies' Press: Tokyo, 1981.

(37) Turner, D. W.; Baker, A. D.; Baker, C.; Brundle, C. R. *Molecular Photoelectron Spectroscopy, A Handbook of He 584 Å Spectra*; Interscience: London, 1970.

(38) Dunbar, R. C. In *Gas-Phase Ion Chemistry*; Bowers, M. T., Ed.; Academic: New York, 1979; vol. 3, Chapter 20.

(39) Woodward, R. B.; Hoffmann, R. *The Conservation of Orbital Symmetry*; Verlag Chemie: Weinheim, Germany, 1970.

(40) March, J. *Advanced Organic Chemistry: Reactions, Mechanisms, and Structure*; McGraw-Hill: Tokyo, 1977.

(41) Lifshitz, C. *Acc. Chem. Res.* **1994**, *27*, 138.